ORIGINAL PAPER

Synchronization modulation of Na/K pump molecules can hyperpolarize the membrane resting potential in intact fibers

Wei Chen · Robin Dando

Abstract Previously, we have theoretically studied the possibility of electrical rhythmic entrainment of carrier-mediated ion transporters, and experimentally realized synchronization and acceleration of the Na/K pumping rate in the cell membrane of skeletal muscle fibers by a specially designed synchronization modulation electric field. In these studies we either used cut fibers under a voltage clamp or intact fibers, but in the presence of ion channels blockers. A question remained as to whether the field-induced activation observed in the pump molecules could effectively increase the intracellular ionic concentration and the membrane potential at physiological conditions. In this paper, we studied the effects of the field on intact fibers without any channel blockers. We monitored the field-induced changes in the ionic concentration gradient across the cell membrane and the membrane potential non-invasively by using a fluorescent probe and confocal microscopic imaging techniques. The results clearly show that the entrainment of the pump molecules by the synchronization modulation electric field can effectively increase the ionic concentration gradient, and hence, hyperpolarize the membrane potential.

Keywords Na/K pump molecules · Electric field · Synchronization · Modulation · Skeletal muscles · Intact fibers

Introduction

The Na/K pump molecule extruding three Na ions out of the cell by exchanging two K ions and consuming one ATP

W. Chen (✉)· R. Dando
Cellular and Molecular Biophysics, University of South Florida,
Tampa, FL 33620, USA.
e-mail: wchen@cas.usf.edu

molecule, is one of the most prevalent active transporters in living systems. The pump molecules are critical to many cell functions such as signal generation, energy supply, and homeostasis. Pathophysiological changes in the density of pump molecules and dysfunctions in their activity are often involved in many diseases (Clausen, 1998, 2003). Moreover, the Na/K pumps consume about 20–80% of the cell's resting metabolic energy depending on the extent of electrical activity of the tissue (Lauger, 1996). Therefore, the Na/K pump molecules have become a central target for both acute and long-terms regulations in therapeutic intervention.

Due to the involvement of ion-transports across the cell membrane, functions of the Na/K pumps are sensitive to the membrane potential. Significant efforts have been made to electrically regulate or activate the pump functions. Pioneering work by Tsong and Tissies (Teissie and Tsong, 1980) used a megahertz oscillating electric field to activate the Na/K pump molecules in erythrocytes. Blank and Soo (1989, 1990) have reported that an AC current can either stimulate or inhibit ATP hydrolysis activity of the enzymes, depending on the ratio of Na and K ions. Several theoretical models have been postulated for the mechanisms involved in electrical activation of the enzymes, including the resonance frequency windows model in which an oscillating electric field can activate the pump functions (Markin et al., 1992; Robertson and Astumian, 1991), the Brownian motion model (Astumian, 1997; Tsong, 2002) and the adiabatic pump model (Astumian, 2003). The studies did not give detailed information such as the locations, widths, and numbers of the frequency windows, but kilohertz (Markin et al., 1992) and megahertz bands were implied (Robertson and Astumian, 1991). All of these studies share a common focus, using an electric field with a fixed frequency, which implies that the process of energy absorption from an electric field is a transient event.

We recently developed a new technique: dynamic entrainment of the Na/K pump molecules (Chen, 2006a, 2006b; Chen and Zhang, 2006; Chen and Dando, 2006). Instead of a transient event, we considered that activation of the pump functions is a procedure of electrical entrainment of the pump molecules. The entrainment consists of two steps: synchronization, forcing all of the pump molecules to work at the same pace; and then, modulation, gradually modulating the pump molecules to higher and higher pumping rates. We have designed a synchronization modulation electric field, and realized electrical entrainment of the Na/K pump molecules, monitored by directly measuring the pump currents. In the study of intact fibers using fluorescent micro-imagining techniques we have shown that the electric field can effectively increase the cell ionic concentration gradients and hyperpolarize the membrane potential. However, all of these experiments were conducted not under physiological condition, either under a voltage clamp or in the presence of various channel blockers.

In this paper, we tested this technique by using intact fibers in physiological solution without any channel blockers. The applied electric field inevitably had some effects on other membrane proteins such as opening ion channels resulting in a decrease in ionic concentration gradient and a depolarization in the membrane resting potential. The goal of this study is to test whether under physiological conditions, the synchronization modulation electric field can effectively reinstate and even increase the ionic concentration gradient and the membrane potential.

Methods and materials

Selection of fluorescent dye

Tetra Methyl Rhodamine Ethyl Ester, TMRE (Fig. 1), a Nernstian dye was used in observing changes in the ionic concentration gradient and the membrane potential. The lipiphilicity of the dye, combined with the delocalization of the molecule's positive charge allows TMRE to pass through the membrane with ease, resulting in good membrane permeability (Sims et al., 1974; Waggoner, 1979). Due to its cationic state, TMRE molecules will be drawn into the cells due to negative potential. In contrast to many fluorescent dyes which exhibit fluorescence only when binding with specific molecules resulting in structural rearrangement, typically involving charge shift, TMRE will always fluoresce. The high permeability allows TMRE redistribution across the membrane when the membrane potential changes. Therefore, by measuring the fluorescence intensity ratio inside over outside the cell, the membrane potential can be calculated via the Nernst equation (Sims et al., 1974; Waggoner, 1979):

$$V_n = \frac{RT}{z_n F} \ln \left(\frac{c_n^o}{c_n^i} \right)$$
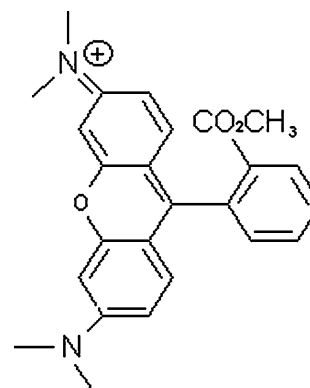
Fig. 1 Structure of slow Nernstian dye, TMRE

When the muscle fibers are exposed to an oscillating electric field, the field-induced oscillating membrane potential will be superimposed on the membrane resting potential. This fast oscillating component is not of interest to us except when calibrating the magnitude of the membrane potential. We mainly focus on the slow changes in the membrane resting potential, or the DC component. Activation of the pump molecules slowly increases the ionic concentration gradient across the cell membrane, and hence, gradually hyperpolarizes the membrane potential. Then, it takes time for the dye molecules to be redistributed throughout the cells. The Nernstian dye, TMRE, a so called slow dye, fits our requirements very well.

Moreover, in contrast to fast potential dyes showing low sensitivity to the membrane potential, slow dyes tend to exhibit superior potential sensitivity in comparison with their faster counterparts. For example, fast dyes such as di-4-ANNEPS, or di-8-ANEPPS, show approximately only as high as a 10% change in response to a membrane potential variation of 100mV. TMRE shows orders of magnitude higher fluorescence under a similar potential change.

Other factors which make this dye an ideal choice for this application are that its spectral properties are independent of environment (Loew, 1993), and that it carries a low rate of phototoxicity (Tsien and Waggoner, 1990). Analysis using TMRE is not carried out ratiometrically, as the spectral properties of TMRE do not change significantly as a result of changes in factors such as pH, or in our case, membrane potential.

Fiber preparation and confocal imagining

Since skeletal muscle contains one of the major pools of the Na/K pumps, we used intact fibers from skeletal muscles. Twitch skeletal muscles, *semitendinosus* and *ilio*, were hand dissected from the leopard frog *Rana Pippiens*, in relaxing solution as in prior work (Hille and Campbell, 1976; Irving et al., 1987; Chen and Wu, 2002). The fibers were held in a

custom-made chamber by two clips with a distance of about 3 mm. A coverslip was placed on top of the two clips in order to reduce the depth of the bathing solution around the fiber. The purpose of this is to increase the resistance of the bathing solution in order to reduce Joule heating effects. Finally, the fibers were stained with 0.8 μM of TMRE in Normal Ringer solution.

TMRE molecules were gradually drawn into the cells due to the negative membrane potential. If using a concentration over a threshold and on a sufficiently long timeline the dye will eventually settle within the cell's mitochondria. Our staining time and dye-concentration were suitably low for the fluorescence to remain representative of the cell's membrane potential.

The experiments were conducted using a confocal microscope to observe changes in the cell's spectrofluorescent image when exposed to the synchronization modulation electric field. An Olympus IX81 inverting, fully computer-controlled confocal microscope utilizing the Fluoview 500 Tiempo V4.3 analysis package was employed for data collection, with a 10x dry objective and a confocal aperture of 80 nm giving a resolution in the X and Y directions of 0.621 μm, and a Z resolution of 3.09 μm. Standard Rhodamine optics of excitation under a green HeNe at 543 nm and detection with a photomultiplier and barrier filter at 560 nm were employed to graph the observed Fluorescence as a two dimensional map, varying with time.

The synchronization modulation electric field was generated by a modified function generator, TENMA UTC 72-5085 and applied to the fiber by connecting to two Ag/AgCl wires parallel in the chamber. The small cross-section of the bathing solution surrounding the fiber comparing to the distance between the two wires of about 1 cm makes the applied electric field relatively uniform.

Two kinds of electrical fields were used in our experiments: a frequency of 50 Hz stimulation and the synchronization modulation stimulation. Both stimulations are ac square-pulsed waveforms with a potential of 8 V, peak-to-peak, which generated a field strength of 8 V/cm. For a fiber with a diameter of 100 μm, the field induced membrane potential was estimated as 40 mV, peak-to-peak. The waveform of the synchronization modulation electric field has been described previously (Chen and Zhang, 2006; Chen and Dando, 2006).

Because of it consisting of thousands of pulses, it is difficult to draw the waveform in a figure. The principle in design of the field is described as follows: There were two steps in the stimulation. The first step is to apply an oscillating electric field with a frequency comparable to the pumps' turnover rates to synchronize the pump molecules to work at the same pace. Therefore, the two half-cycles of the oscillating electric field can alternatively facilitate the Na- and K-transports to reduce the time needed for each pumping loop. By gradually and slowly increasing the field frequency and retaining the pump synchronization, the pumping rate will follow the frequency changes. As a result, the pump molecules can be modulated to higher and higher pumping rates. In our experiments, the synchronization stimulation consists of a 50 Hz pulse-train. Our previous results showed that a 50 Hz oscillating electric field can synchronize the pump molecules. After a finite duration, the frequency was slowly increased in a step of 1%, finally researched a value of 200 Hz, and then, remained at this value until removal of the field. Synchronization and modulation of the Na/K pumps has been theoretically investigated (Chen, 2006a, 2006b) and experimentally demonstrated previously (Chen and Zhang, 2006; Chen and Dando, 2006).

The compositions of solutions are as follows:

Relaxing solution – 120 mM K-Glutamate, 5 mM K_2PIPES, 1 mM $MgSO_4$, 0.1 mM K_2EGTA.
Ringer solution (Normal Ringer solution) – 120 mM NaCl, 2.5 mM KCl, 2.15 mM Na_2HPO_4, 0.85 mM NaH_2PO_4, 1.8 mM $CaCl_2$.

Dye solution, same as the ringer with 0.8 μm TMRE. All solutions were titrated to a working pH of 7.0.

Results

After the fluorescent intensity inside the cell became stable, indicating establishment of a steady-state which usually took 20 min, the 50 Hz stimulation field was applied to the fibers for about 2 min. A narrow data acquisition box (5 × 40 μm) was placed at the intracellular side near (5 μm away from) the cell membrane with the long edge along the membrane. Fluorescent images in the box were continuously recorded. The averaged fluorescent intensities in the box were plotted as a function of time shown in Fig. 2. The vertical dotted line represents the starting time of the stimulation. It is clear that the stimulation field caused a decrease in the intracellular fluorescent intensity from 1540 to 1370 units. This decrease can be attributed to the channel opening elicited by the 50 Hz stimulation. Leakage currents though the ion channels cause a reduction in the intracellular ion concentration, and hence, depolarize the membrane potential.

After removal of the field, the fiber was relaxed until the fluorescent intensity was fully recovered. Then, the synchronization modulation electric field was applied to the fiber, again, for 2 min. With an initial frequency of 50 Hz for 5 s, the frequency was gradually increased to 200 Hz in 30 s, and then remained at this value for about 80 s. During the field application, fluorescent images around the cell membrane were continuously taken. The fluorescence intensities recorded in the same data-acquisition box described above were averaged, and are plotted in Fig. 3 vs. time. Again,

## Localised Fluorescence response to Stimulation of Fibre
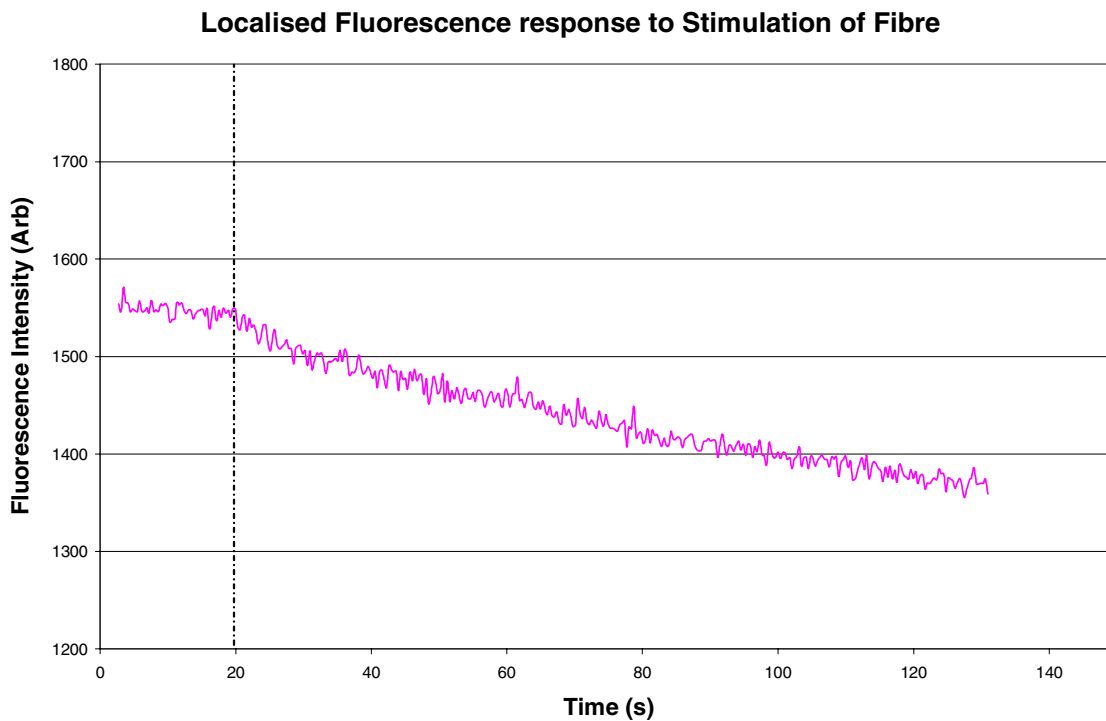
Fig. 2 Fluorescent intensity near the cell membrane was reduced due to a stimulation of 50 Hz pulse-train for 2 min. The ordinate is fluorescent intensity in arbitrary units. The stimulation field was applied at 20 s shown as a vertical line

the field was applied at the vertical line. Similar to those shown in Fig. 2, the fluorescent intensity was reduced at an early stage. Interestingly, after reaching a minimal value, the fluorescent intensity began to increase. In about 30 s, the intensity reached the original value of 1540 units, and then continuously increased to 1700 units.

By comparing the two traces shown in Figs. 2 and 3, the two stimulations induced changes in the fluorescent

Localised Fluorescence response to Stimulation of Fibre with Modulation
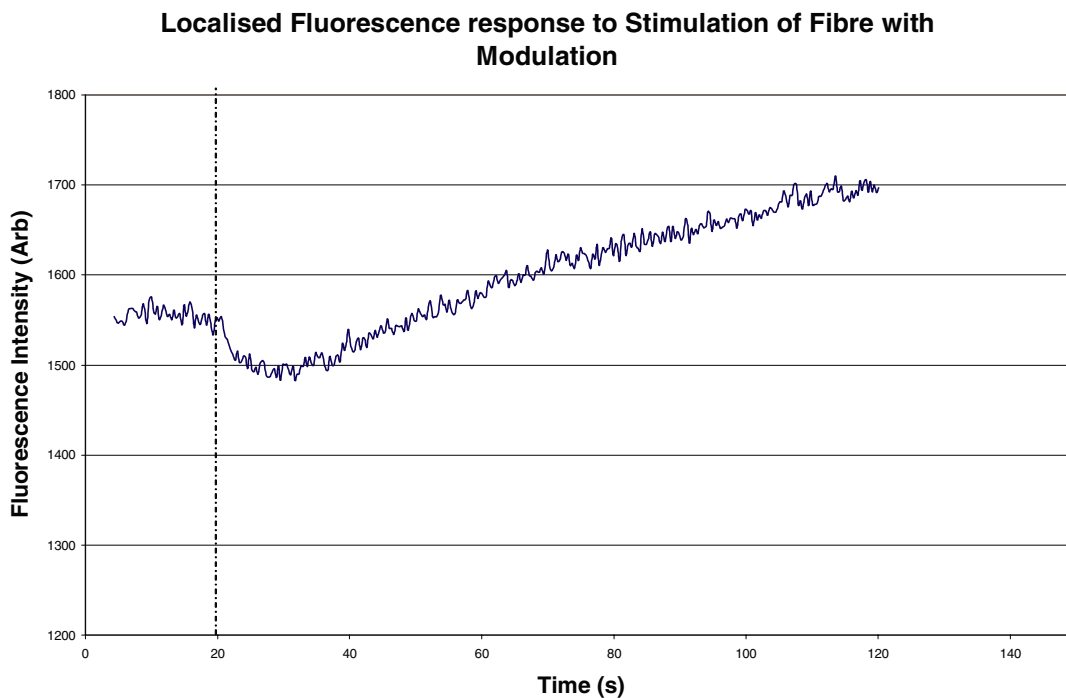
Fig. 3 The synchronization modulation electric field induced changes in the fluorescent intensity using the same protocol of Fig. 2

Localized fluorescence variation after application of stimulation and Modulation electric field at 20s
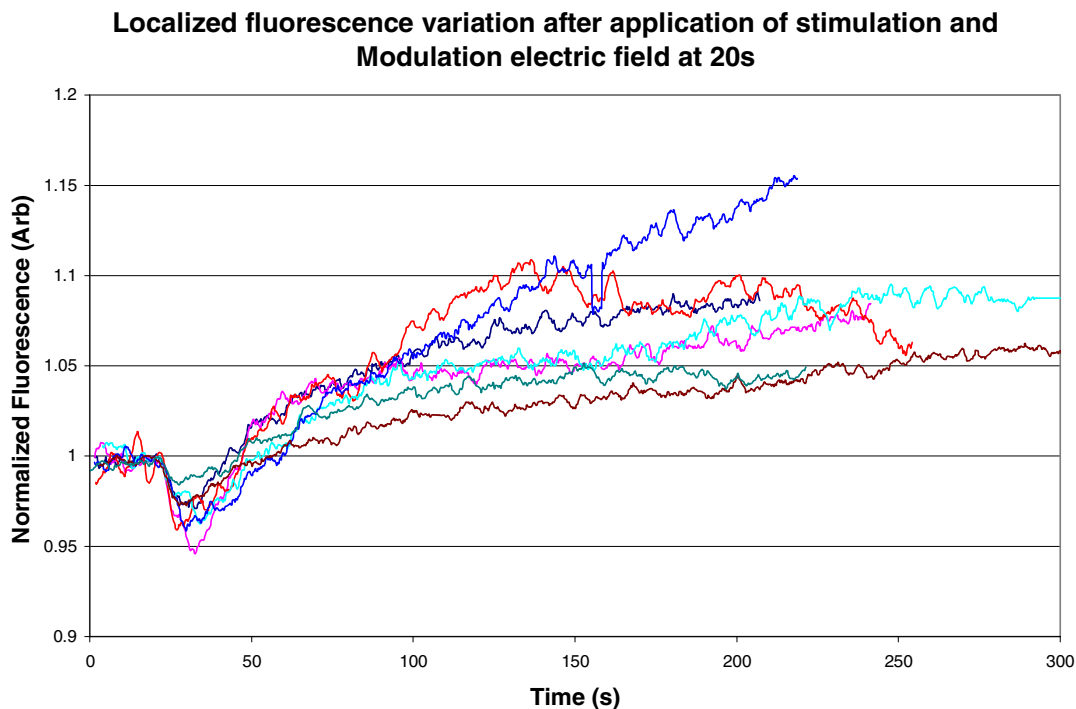
Fig. 4 Results from seven experiments. The recorded fluorescent intensities were normalized to the original values before the field application, respectively. Again, the fields were applied at 20 s

intensity differ significantly. The 50 Hz stimulation decreased the intensity. Thereafter, the fluorescent intensity gradually recovered to, but never higher than, the original value in a relatively long time, quite a few minutes. In contrast, the synchronization modulation electric field, despite briefly decreasing the fluorescent intensity at an early stage, not only quickly reinstated the intensity, but also significantly increased it.

Seven experiments were conducted using the same field and protocol. The fluorescent intensities were normalized to the original value before the field application, respectively, and are plotted as functions of time shown in Fig. 4. The results consistently show the same pattern: after a brief decrease at the early stage, the fluorescent intensity started to increase, and could reach a value even higher than the original one. The statistics of the traces are shown in Fig. 5. The bars represent the standard deviation. The averaged increase in the fluorescent intensity for seven fibers is 7% after 2.5 min application of the synchronization modulation electric field.

We also studied the field-induced changes in the intracellular fluorescent intensity at the region away from the cell membrane. Two data acquisition boxes were employed. One was, as described above, $5 \times 40 \ \mu$m, and another is $20 \times 40 \ \mu$m. Both boxes were put as close as possible to the cell membrane with a long edge along the membrane. The fluorescent intensities recorded in both boxes were averaged,

respectively, and are plotted as functions of time shown in Fig. 6. The lighter trace represents the fluorescence in the narrow box which shows a relative larger decrease at early stage but later larger increase than those obtained from the wide box shown as the darker trace. If comparing the lighter trace in Fig. 6 with the trace in Fig. 5, even though the sizes of the data acquisition boxes are the same, the closer the box was put to the membrane, the larger the effects which can be observed.

Because the resistivity of cell membrane is much larger than that of both intracellular and extracellular electrolytes, the overwhelming majority of the field-induced potential was across the cell membrane which affected the membrane proteins. Either opening the ion channels or activating the pump molecules, the region near the cell membrane shows more significant effects than those in distant regions.

We further investigated how the synchronization modulation electric field affects the distribution of the fluorescent intensity throughout the fibers. We took images crossing the entire fiber diameter before, during, and after the application of the electric field. The left panel in Fig. 7 is a slice image taken before the application of the electric field. The horizontal line indicates the location of the fluorescent intensities measured. The dye intensities recorded from the image taken before the field application were plotted throughout the fiber diameter, shown as trace 0 in the right panel of Fig. 7, where the abscissa axis is in units representing the pixel number.

Statistics of Fluorescence Variation after Application of Synchronization/Modulation Field
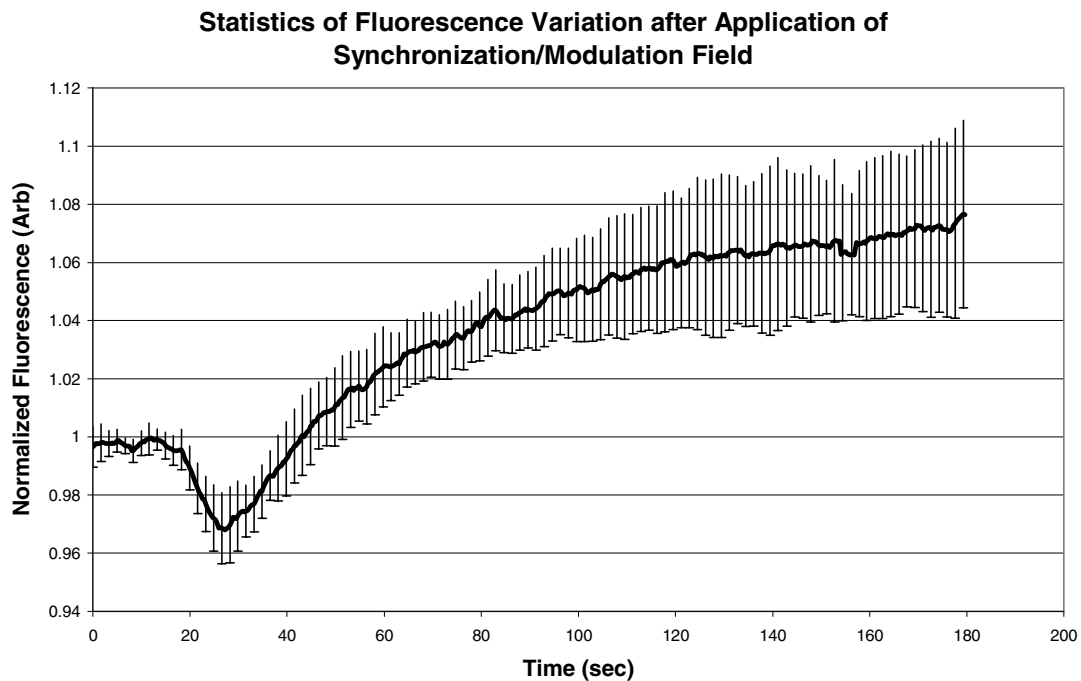
Fig. 5 Statistics of the seven traces shown in Fig. 4. The bars represent standard deviation. After 3 min application of the synchronization modulation electric field, the averaged increase in the fluorescent intensity was 7%

It is necessary to point out the dye intensity graph has been smoothed to eliminate the fluctuation effects of fluorescence arising from interior organelles in the fiber. The smoothing function is a simple averaging of fluorescence across the fiber. In close proximity to the cell membrane the averaging is applied unidirectionally to ensure no artificial smoothing of the areas around the membrane boundary. It is clear that the fluorescent intensity inside the cell is significantly higher

Dye Intensity Response to Stimulation and Modulation
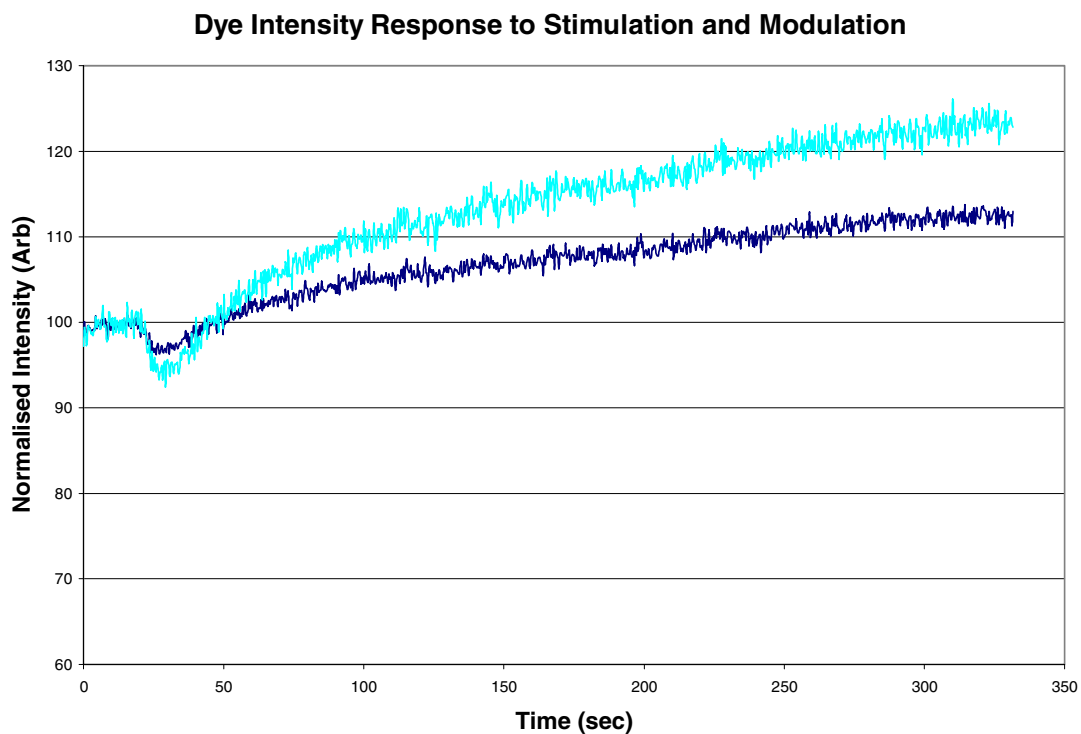
Fig. 6 The synchronization modulation electric field-induced changes in the fluorescent intensity recorded in two boxes: $5 \times 40 \ \mu$m (light trace) and $20 \times 40 \ \mu$m (dark trace) put as close as possible to the cell membrane with the long edges along the membrane

Fluorescence Intensity during stimulation and modulation of Pump Molecules
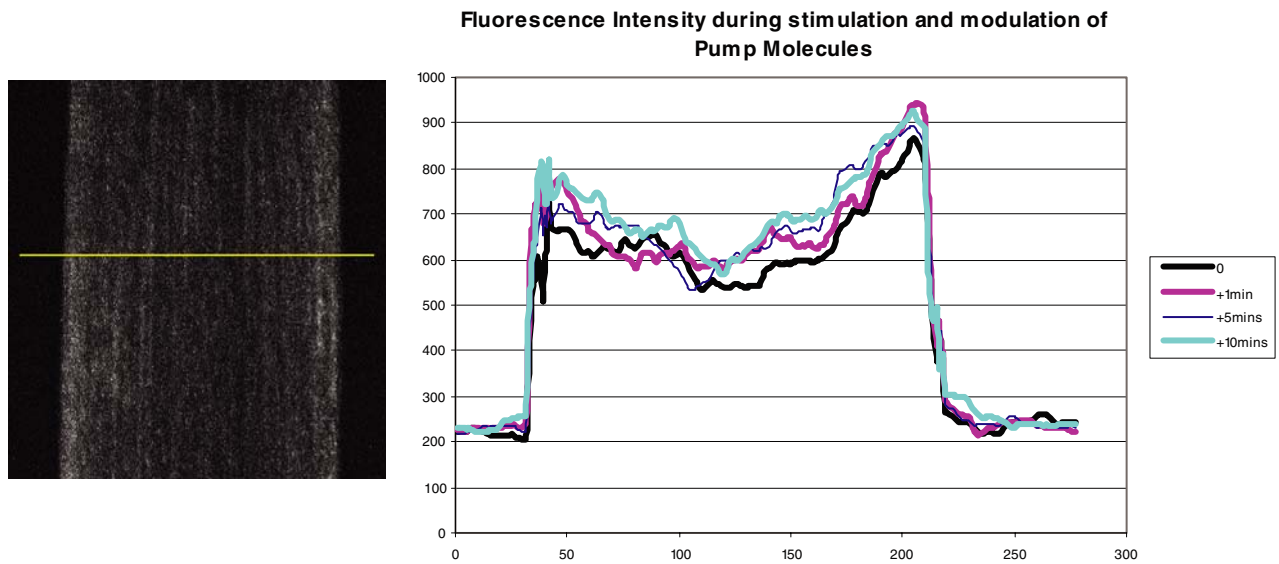
Fig. 7 Fluorescence intensity distributions throughout the fiber. Left panel: a slice image of a skeletal fiber. The horizontal line represents the location of the fluorescent intensity measured throughout the fiber. Trace 0 min was taken right before the electrical stimulation. Then the synchronization modulation electric field was applied to the fibers for 5 min. Traces 1 min, 5 min, and 10 min were taken 1, 5 and 10 min after the electric field started to be applied, respectively

than that outside the cell due to the intracellular negative membrane potential.

Then, the synchronization modulation electric field was applied to the fibers for 5 min. At the end of the first minute of the field application, the fluorescent image was retaken. The measured fluorescent intensity across the fiber was shown as trace 1 min in the figure. By comparing this trace to that taken before the field application, the intensity elevation was mainly near the membrane boundary showing a localized increase in the ionic concentration, while those away from the membrane remained relatively unchanged. This result is consistent to those shown in Fig. 6, only the region near

the cell membrane showing noticeable effects. An additional 4 min later, immediately following the removal of the electric field, the fluorescent intensity was re-measured and the results are shown as trace 5 min. It indicates a further increase in the dye intensity, and gradual redistribution throughout the cell. Finally, an image was taken 5 min after the removal of the electric field, and the fluorescent intensity is shown as trace 10 min. It shows a relative uniform increase throughout the fiber. The dye concentration is noticeable higher than that of the initial scan, indicating an increase in the ionic concentration of the whole cell.

Fig. 8 The result from the same experiment shown in Fig. 7 except 1 mM ouabain was applied in the bathing solution. No discernable changes can be observed in response to the field application

Stimulation and modulation in presence of Ouabain
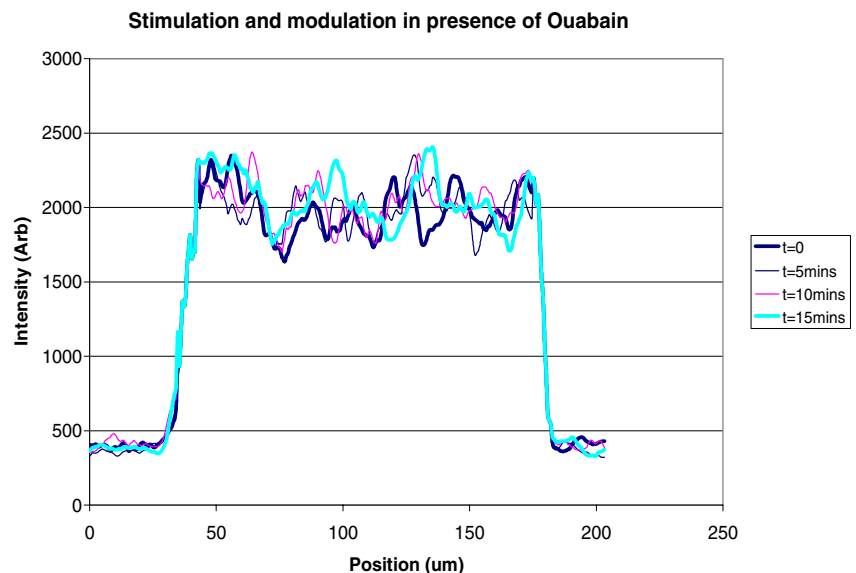
Fig. 9 Global fluorescent intensities measured across the whole fiber diameter starting from the staining of the fiber. The synchronization modulation electric field was applied to the fiber during the period between two vertical lines. With some time-delay, the field increased the fluorescent intensity

Whole Cell Fluorescence response to Stimulation and Modulation Field
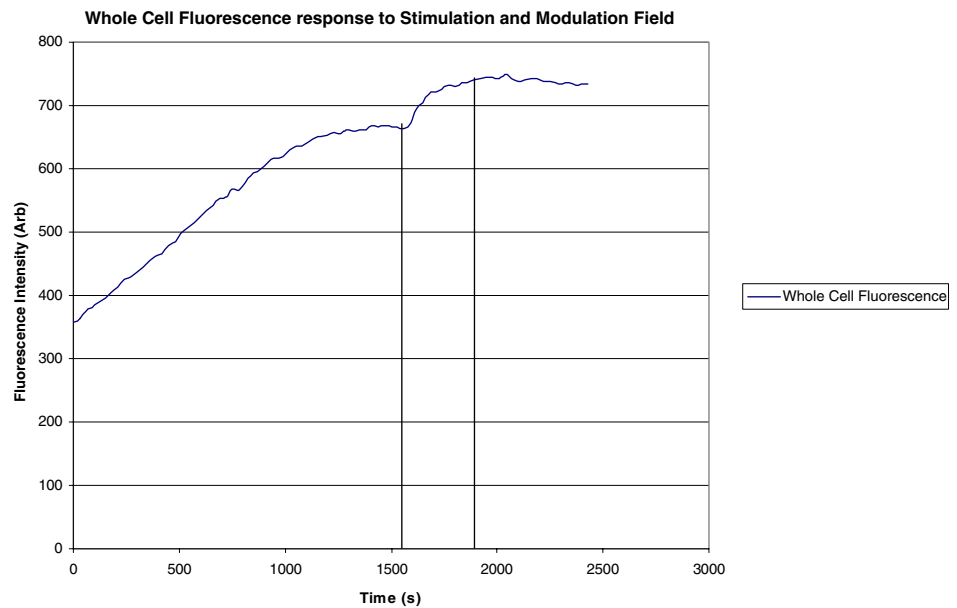
The averaged fluorescent intensities across the fiber are estimated about 630 and 730 arbitrary units before and after the electrical stimulation, respectively. The outside intensity remains a constant 230 units. After subtracting the background, the potential difference across the cell membrane was estimated according to Eq. (1) as -79 mV for the control, and increased to around -85 mV after 5 min stimulation.

In the course of our previous studies we have theoretically predicted (Chen, 2006a, 2006b) and experimentally proved (Chen and Zhang, 2006; Chen and Dando, 2006) that the synchronized modulation electric field can significantly accelerate the pumping rate of the Na/K pump molecules. Activation of the pump molecules means more K ions can be pumped into the cell resulting in a higher intracellular K concentration and a higher polarized membrane potential. To verify that the field-induced changes in membrane potential were due to activation of the Na/K pump molecules, we repeated the above experiment with 1 mM ouabain in the bathing solution. With the same protocol, the fluorescent intensities throughout the fiber were measured and are plotted in Fig. 8.

All of the four traces, taken before, during, and after the application of the synchronization modulation electric field, show a similar profile of fluorescent intensity across the fiber. The absence of a discernable variation in the fluorescence means that the field had no effects on the membrane potential due to the presence of ouabain. This result proved that the field-induced increase in the intracellular fluorescence intensity was ouabain-sensitive, or due to activation of the Na/K pumps.

In addition to the use of ouabain to inhibit the pump molecules, we also repeated the experiments in potassium-free bathing solution in order to eliminate the pump currents.

Again, all of the intracellular fluorescent intensities taken before, during, and after the field application showed a similar profile throughout the fibers. These results further confirmed that the oscillating electric field-induced increases in the intracellular fluorescent intensity were solely due to activation of the Na/K pumps.

Finally, we monitored the global changes in intracellular fluorescent intensity as a function of time induced by the application of the synchronization modulation electric field. Images of whole cross sections of the fiber were continuously taken after changing the bathing solution to stain the fibers. The averaged fluorescent intensity throughout the fiber was plotted as a function of time shown in Fig. 9. Starting from staining, the fluorescent intensity shows an exponential-like increment until reaching a plateau, representing a steady-state of the fluorescent dye across the cell membrane. This typically took over 20 min, due to slow diffusion and large cell dimensions.

Then, the synchronization modulation electric field was applied to the fibers between the two vertical lines. With some time delay, the fluorescent intensity of the dye molecules started to increase until removal of the electric field.

In Fig. 9, it does not show the initial decrease in the fluorescent intensity at the early stage of the field application as showed in Figs. 3–6. That is due to two reasons. First, the fluorescent intensities plotted here are averages through the fiber diameter. Stimulation-induced transient reductions in the ionic concentration gradient due to channel opening only occur in the region close to the cell membrane. Secondly, the time-interval of taking images was 1 min which is much longer than that for the traces shown in the previous figures.

Discussions and conclusions

In this study, we tested the synchronization modulation electric field on intact fibers to build up ionic concentration across the cell membrane in physiological solution without any channel blockers. When an intact fiber is exposed to the electric field, in addition to activating the Na/K pumps, the electric field inevitably affects other membrane proteins, such as opening ion channels. The transient channel currents which are passive currents reduce the ionic concentrations gradient across the cell membrane. Our results showed that with a well designed synchronization modulation electric field, activation of the pump functions is able to compensate for those channel-opening induced side-effects.

The underlying mechanisms involved in this process may be discussed as follows: Indeed, magnitude of the channel current is much larger than that of the pump currents. However, pumps run continuously all of the time in contrast to a transient opening of the ion channels. In fact, at physiological conditions, a relatively stable membrane resting potential indicates that continuous work of pump molecules is able to compensate for the transient channel currents. Considering the 4-fold increase in the pumping rate, it is reasonable to observe building up the ionic concentration gradient.

In addition, inactivation of the ion channels may play a significant role. It is well known that the voltage-dependent Na channels have characteristic inactivation features. Our results in study of Na channels showed that the refractory period was significantly prolonged when the cell membrane was repeatedly stimulated. After a certain number of stimulations, the Na channels were almost fully inactivated, and very little channel currents could be measured (Chen and Zhang, in press). In terms of delayed rectifier K channel, their slow kinetics of the channel currents indicates a minimum requirement in the duration of stimulation in order to open the channels. When the duration is shorter than that limit, the stimulation can not fully open the delayed rectifier K channels. In addition, even though inactivation of the delayed rectifier K channels is not as quick as the Na channels, our recent studies in K channel inactivation showed that their refractory period can also be significantly extended in response to repeatedly stimulations. In other words, continuous stimulations also inactivate the K channels (results will be reported separately).

Moreover, in design of the waveform of our electric field, we deliberately increased the modulation rate in a manner that the pump molecules could follow this synchronization at each frequency. Starting from a low synchronization frequency, the channel-opening initially plays a major role resulting in a brief reduction in the ionic concentration near the cell membrane, shown in Figs. 2–6. As the modulation frequency further increases, more channels are either inactivated by the repeatedly stimulations or do not respond to the shorter pulse-duration. On the other hand, the frequency modulation makes the Na/K pumps run faster and faster. As a result, the synchronization modulation electric field is not only able to compensate for the leakage through the ion-channels but eventually builds up the ionic concentration. All these effects are fully eliminated in the presence of ouabain.

Combined with our previous results showing that the synchronization modulation electric field can activate the Na/K pumps (Chen, 2006a, 2006b; Chen and Zhang, 2006; Chen and Dando, 2006), this study provides evidence that the field-induced pump activation can compensate for the side effects inevitably induced by the electric field on other membrane proteins. All these studies consistently show that by activating the pump functions, the synchronization modulation electric field can effectively manipulate or control the intracellular ionic concentration at physiological conditions, and even build up ionic concentration gradients across the cell membrane and hyperpolarize the membrane potential.

Comparison of the underlying mechanisms involved in this technique and those in prior work

As mentioned in the introduction, significant efforts have been made in the study of electrical activation of Na/K pumps using an oscillating electric field. An excellent review paper by Tsong (Tsong, 1990) summarized the potential mechanisms involved in pump-activation. In general, this work is based on these studies to further investigate electroconformational changes in the pump molecules, even though the underlying mechanisms, including the assumptions, targets of the protein's structures, and the expected results are different from those studies.

In those studies, a fundamental assumption is the existence of one or more intrinsic oscillating frequency of the pump molecules. Therefore, when the frequency of an oscillating electric field fell into these intrinsic or optimal frequency window(s), the electric field can resonate with, and enforce the pumps' conformational oscillation. In contrast, in our study, no assumption about the intrinsic oscillating frequency was made. Instead, we assume that the turnover rates of the pumps conformational change are adjustable.

Secondly, in the previous study, even though the location of the optimal frequency windows was not specified, it was implied up to a range of MHz. Therefore, the target of the electric field is most likely not on the whole pump molecules, because of their much lower turnover rate (in tens of Hz) than the MHz frequency window(s), but on some specific transient steps or sub-steps in the pumping loop. In contrast, we are focusing on the turnover rate of the whole pump-molecules, and activating the pumping rate of the entire loop instead of on specific steps. Therefore, the initial frequency we applied to the cells is always comparable to the natural turnover-rates of the pump molecules.

Thirdly, the mechanisms involved are different. Indeed, the resonance-frequency model also implies synchronization of the pump molecules by the AC field. The synchronization or resonance field can enforce the pumps' conformational oscillation, and therefore, activate their functions. In our study, the synchronization is only the first step in the technique, which does not activate the pump functions. We consider activation of the pump molecules as an entrainment procedure of the pump molecules, which consists of two steps: synchronization and modulation. First, based on the fact that individual pumps work independently with different turnover rates and random turnover phases, we apply an oscillating electric field with a frequency comparable to their turnover rates in order to force them to pump at the same pace. Our voltage clamp studies showed that the synchronized pump molecules were entrained to the same pumping pace, extruding Na ions out of the cell at the same time and then pump in K ions thereafter, and showing alternating outward and inward components of the pump currents. At this step, the pump currents were not increased. Once synchronized, the field frequency increases a small amount to synchronize the pumping rate to the new higher frequency. Consequently, the pump molecules can be modulated to higher and higher pumping rates in a stepwise pattern. Our theoretical studies showed that by this method the pumping rate can be facilitated exponentially as a function of the field-strength (Chen, 2006a, 2006b). Synchronization of the pump molecules and modulation of the pumping rate have been demonstrated previously by using the voltage-clamp technique to directly monitor the pump currents (Chen and Zhang, 2006; Chen and Dando, 2006).

Bibliography

Astumian RD (1997) Thermodynamics and kinetics of a Brownian motor. Science 276:917

Astumian RD (2003) Adiabatic pumping mechanism for ion motive ATPases. Phys Rev Lett 91(11):118102(4)

Blank M, Soo L (1989) Bioelectrochem Bioenerg 22:313–322

Blank M, Soo L (1990) Bioelectrochem Bioenergetics 24:56–61

Chen W (2006a) Synchronization modulation of ion-transporter in cell membrane. Phys Rev Lett (submitted, under review)

Chen W (2006b) Voltage-dependence of carrier-mediated ion transport. Phys Rev E (in press)

Chen W, Dando R (2006) Electrical activation of Na/K pumps can increase ionic concentration gradient and membrane resting potential. Biochem Biophys Acta (submitted, under review)

Chen W, Wu WH (2002) The asymmetric, rectifier-like I–V curve of the Na/K pump transient currents in frog skeletal muscle fibers. Bioelectrochemistry 56:199–203

Chen W, Zhang ZS (2006) Synchronization of Na/K pump molecules by a train of squared pulses. J Bioenergetics Biomembranes (in press)

Chen W, Zhang ZS (in press) Repeated stimulations can prolong the refractory period of the voltage-gated Na channels. Biophys J (submitted, under review)

Clausen T (1998) Clinical and therapeutic significance of the Na, K pump. Clin Sci 95:3–17

Clausen T (2003) Na/K pump regulation and skeletal muscle contractility. Physiol Rev 83:1269–1324

Hille B, Campbell DT (1976) An improved Vaseline gap voltage clamp for skeletal muscle fibers. J Gen Physiol 67:265–293

Irving M, Maylie J, Sizto NL, Chandler WK (1987) Intrinsic optical and passive electrical properties of cut frog twitch fibers. J Gen Physiol 89:1–40

Lauger P (1996) Electrogenic pump molecules

Loew LM (1993) Confocal microscopy of potentiometric fluorescent dyes. Meth Cell Biol V38:195–209

Markin VS, Liu DS, Rosenberg MD, Tsong TY (1992) Resonance transduction of low level periodic signals by an enzyme: an oscillatory activation barrier model. Biophys J 61(4):1045–1049

Robertson B, Astumian D (1991) Frequency dependence of catalyzed reactions in a weak oscillating field. J Chem Phys 94(11):7414–7418

Sims PJ, Waggoner AS, Wang CH, Hoffman JF (1974) Studies on the mechanism by which cyanine dye measure membrane potential in red flood cells and phosphatidylcholine vesicles. Biochemistry V13:3315–3330

Teissie J, Tsong TY (1980) Evidence of Voltage-induced channel opening in Na/K ATPase of human erythrocyte membrane. J Membrane Biol 55:133–140

Tsien RY, Waggoner AS (1990) Fluorophors for confocal microcopy, in "Handbook of Confocal Microscopy," 169–178.

Tsong TY (1990) Electrical modulation of membrane proteins: Enforced conformational oscillations and biological energy and signal transductions. Ann Rev Biophys Biophys Chem 19:83–106

Tsong TY (2002) Na,K-ATPase as A brownian motor: Electric field-induced conformational fluctuation leads to uphill pumping of cation in the absence of ATP. J Biol Phys 28(2):309–325

Waggoner AS (1979) Dye indicators of membrane potential. Annu Rev Biophys Bioeng V8:847–868